IOP Conf. Series: Materials Science and Engineering **1327** (2025) 012210 doi:10.1088/1757-899X/1327/1/012210

Thermomechanical properties and irradiation induced aging of SLA and FDM 3D printed high performance polymers

Christian Scheuerlein[1*], David Mate Parragh[1], Julia Vielhauer[1], Anders Gaarud[1], Noemie Martin[1], Roland Piccin[1]

[1] European Organization for Nuclear Research (CERN), Esplanade des Particules 1, 1211 Geneva, Switzerland

*E-mail: Christian.Scheuerlein@cern.ch

Abstract. The thermomechanical properties of 3D printed polymers for potential use in superconducting devices have been compared. The FDM printed thermoplastics PEEK and ULTEM 9085 exhibit strongly anisotropic properties, with very high mechanical strength and fracture toughness in the flat and on edge printing directions, but much lower strength and toughness in the upright position. FDM printed PEEK exhibits comparatively good radiation hardness, with a moderate degradation of mechanical properties up to a dose of 10 MGy absorbed in ambient air. Among the SLA printed thermosetting resins RG35 has outstanding irradiation hardness, retaining comparatively good mechanical properties up to a dose of 10 MGy.

1. Introduction

3D printing of high-performance polymers enables the production of functional components with complex geometries that cannot easily be obtained by conventional manufacturing methods. In the present study we have characterised the mechanical properties at room temperature (RT) and at 77 K of the two UV curable thermosets Accura 25 and RG35 printed by stereolithography (SLA), and of the thermoplastics ULTEM 9085 and PEEK printed by Fused Deposition Modelling (FDM). To qualify these materials for use in particle accelerators and detectors, where the materials are exposed to ionising irradiation, we compare the thermomechanical properties of the different SLA and FDM polymers before and after gamma irradiation.

2. Experimental

2.1 The samples

In the present study the mechanical properties and radiation hardness of two thermosets, Accura 25 from 3D systems [1], and Ultracur 3D RG35 [2], and two thermoplastics for FDM printing have been compared.

Semicrystalline polyetheretherketone (PEEK) has been characterised without and with ceramic fibre reinforcement (so-called Helios PEEK produced by Roboze [3]).

ULTEM™AM9085F by SABIC is a high temperature, amorphous polyetherimide thermoplastic blend [4],[5].

The FDM printed materials have been characterised printed in three different directions, notably flat (xy), on edge (xz) and upright (zx).

2.2 Irradiation
^{60}Co gamma irradiation has been performed with a dose rate of about of 2 kGy/h in ambient air at a temperature of 20-25 °C. For more information about the irradiation and dosimetry see [6].

2.3 DMA
Storage modulus (G′) and loss modulus (G″) were recorded during temperature sweeps with a Dynamical Mechanical Analyser MCR702e from Anton Paar, Graz, Austria. Glass transition temperatures have been derived according to ASTM D 4065, DIN EN ISO 11357 [7],[8], at a frequency of 1 Hz and a temperature ramp of 2 K/min. During the temperature sweeps the thermal expansion of the samples has been measured as described in [9].

2.4 Tensile tests
Tensile tests were performed according to ISO 527 [10], with a gauge length of 30 mm, and a distance between grips of 75 mm. The test speed was 1 mm/min while measuring the tensile modulus in the elastic stress–strain region, and 5 mm/min after passing the yield point.

2.5 Three-point bending tests
Three-point bending flexural tests were conducted with rectangular beams 80 mm×10 mm×4 mm in accordance with ISO 178 [11], with a crosshead speed of 2 mm/min. The flexural modulus is determined as the slope of the linear fit in the strain range 0.05 to 0.25%.

Because of the limited sample volume available during gamma irradiations smaller short beam samples, 40 mm × 10 mm × 4 mm, have been irradiated and tested according to the standard ISO 14130 [12], with Ø=4 mm loading supports, Ø=10 mm bending die and 20 mm span (5 × the sample thickness ± 0.3 mm). Since ISO 14130 is designed for determining the apparent interlaminar shear strength of fibre-reinforced plastic composites, which is not suitable for the given application, the short beam stress was calculated according to ISO 178.

2.6 Fracture toughness tests
Fracture toughness tests were conducted according to ISO 13586 [13]. K_{Ic} values are derived from 3-point bending load-displacement curves of single edge notched bending (SENB) specimens with nominal dimensions of 80 × 10 × 4 mm^3 and a 2 mm wide and 5 mm deep notch produced by a water jet. A fine artificial crack was added with a razor blade. 3-point bending was done with Ø=10 mm loading supports, a bending die with Ø=4 mm and a span length of 40 mm (4 × the nominal sample width), with a crosshead speed of 10 mm/min.

3. Results

3.1 Thermomechanical properties of the non-irradiated samples
Figure 1(a) compares the storage modulus evolution as a function of temperature *G'(T)* of the different 3D printed materials. The SLA printed thermosetting resins have comparatively low T_g, with the glass transition onset close to ambient temperature. In contrast the glass transition onset of the FDM printed thermoplastic resins exceeds 150 °C. In Figure 1(b) the integrated thermal expansion of the same samples in the temperature range 25-75 °C is compared. Differences in thermal expansion behaviour of the different resins above ambient temperature are mainly due to the differences in T_g. Density, hardness, glass transition temperatures and linear thermal expansion coefficients of the investigated materials are summarized in Table 1. The integrated

thermal expansion ($\Delta L/L$) in the temperature range 10 K-293 K of the UV cured Accura 25 epoxy resin is about 13 mm/m [14].

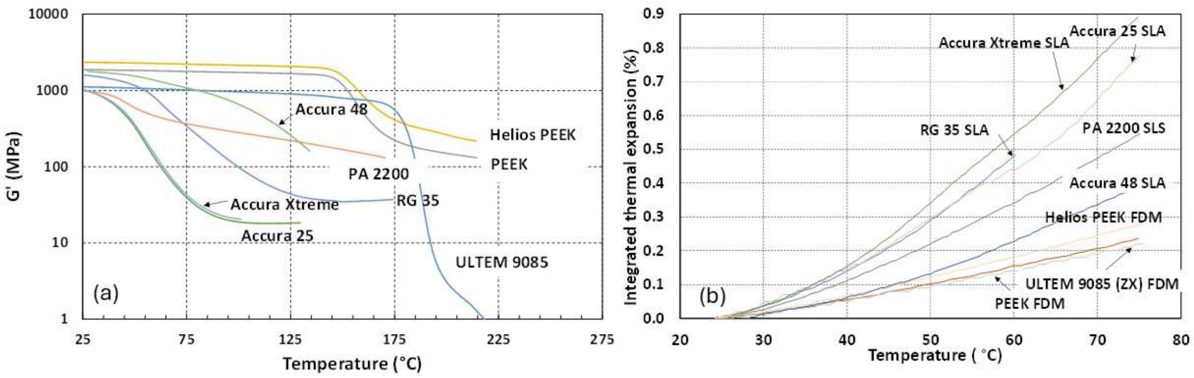

Figure 1. Comparison of (a) storage modulus G' (T) and (b) integrated thermal expansion of SLA, SLS and FDM 3D printed samples. All FDM samples have been printed in upright (zx) direction.

Table 1. Density (ρ) [15], ball indentation hardness (HB) [16], glass transition temperature (T_g), linear thermal expansion coefficient (α) of SLA and FDM printed polymers.

Material	ρ (g/cm^3)	*HB*	T_g *G (°C)*			*α (10^{-6} K^{-1})*
			G' onset	G'' max	tan δ max	25-40 °C
Accura 25	1.21	85±2	20	50	69	97
RG35	1.20	105±3	50	62	88	114
ULTEM 9085 xy	1.24	148±3				47
ULTEM 9085 xz	n.m.	113±20	177	180	190	46
ULTEM 9085 zx	1.19	n.m.				49
PEEK xy	1.29	200±2				43
PEEK xz	1.29	198±6	147	154	160	41
PEEK zx	1.29	218±7				47
Helios PEEK xy	1.46	239±8				27
Helios PEEK xz	1.43	212±3	148	155	162	n.m.
Helios PEEK zx	1.46	233±7				56

3.2 Tensile and flexural properties of the non-irradiated samples

Flexural stress-strain measurements acquired at RT and at 77 K in the different orientations of the FDM printed materials are shown in Figure 2.

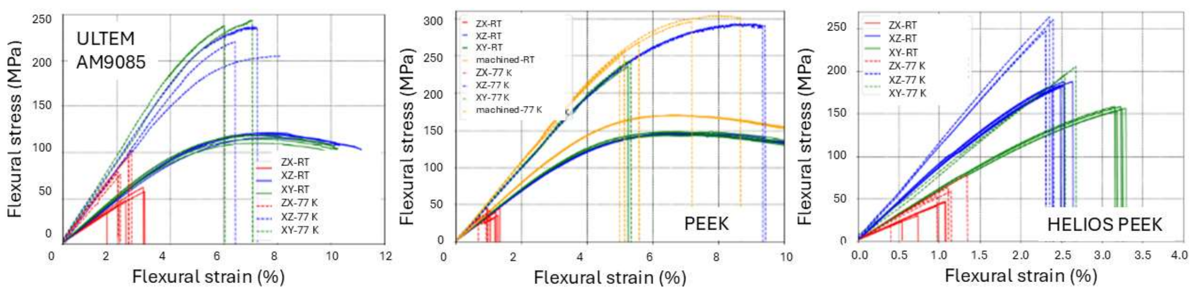

Figure 2. Flexural stress-strain curves of SLA and FDM 3D printed materials at RT and at 77 K. The FDM samples have been printed in three directions. The extruded PEEK is shown for comparison.

The RT and 77 K tensile and flexural properties are summarised in Table 2. The storage modulus (G') has been measured by DMA in torsion mode.

Table 2. Young's modulus (E), flexural modulus (E_f) storage modulus (G'), ultimate tensile strength (σ_m), and flexural strength(σ_{fm}) of SLA and FDM printed polymers at RT and 77 K.

Material	E (GPa)	E_f (GPa)		G' (GPa)	σ_m (MPa)	σ_{fm} (MPa)	
	RT	RT	77 K	RT	RT	RT	77 K
Accura 25	1.4	1.2±0.1	5.5±0.1		24	48±5	81±3
RG35	1.7	2.2±0.1	6.5±0.2		30	82±2	100±5
ULTEM 9085 xy	2.5±0.1	2.5±0.1	4.4±0.1	0.95	80±1	116±3	241±3
ULTEM 9085 xz	2.5±1.3	2.3±0.1	3.9±0.3	0.87	84±1	119±2	220±13
ULTEM 9085 zx	2.2±0.4	2.0±0.1	4.1±0.6	0.84	45±3	49±9	90±11
PEEK xy	3.7±0.5	3.4±0.1	4.9±0.2	1.4	93±2	146±2	241±4
PEEK xz	3.6±0.1	3.3±0.1	4.7±0.1	1.3	93±1	145±1	291±2
PEEK zx	2.7±0.3	3.3±0.1	4.7±0.2	1.4	33±3	37±5	40±6
Helios PEEK xy	6.6±0.3	6.0±0.2	5.3±0.6	2.6	105±4	156±2	186±20
Helios PEEK xz	9.6±0.8	9.0±0.2	11±0.2	1.8	110±9	185±2	258±7
Helios PEEK zx	3.7±0.3	4.2±0.1	5.3±0.6	1.8	13±1	38±9	54±20

3.3 Fracture toughness of the non-irradiated samples

The critical stress intensity factors determined for the thermoplastics FDM printed in xy, xz and zx directions are compared in Figure 3. The fracture toughness in zx directions is comparatively low, similar to that of typical epoxy resins [17]. In xz and xy directions the mechanical strength and toughness are much higher. Adding the ceramic fibres to PEEK has reduced the fracture toughness in all printing directions. The K_{Ic} and G_{Ic} values determined at RT and at 77 K are presented in Figure 3.

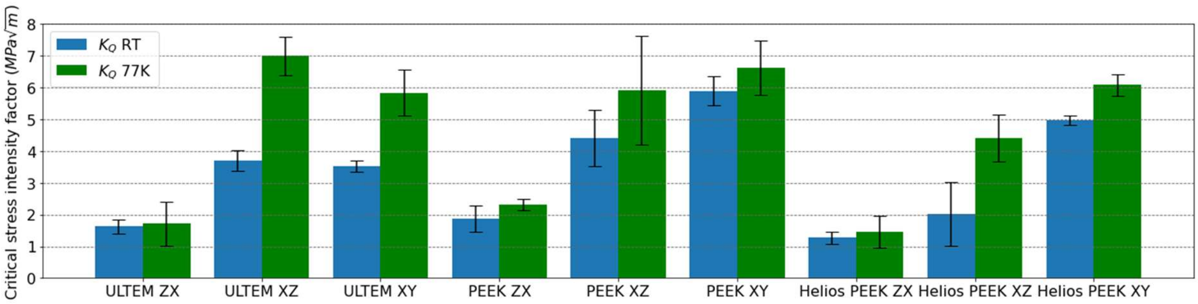

Figure 3. Comparison of critical stress intensity factors of ULTEM AM9085F, PEEK and Helios PEEK printed in zx, xz and xy directions, at RT and 77 K.

Table 3. Critical stress intensity factor (K_{Ic}) and critical energy release rate (G_{Ic}).

Material	K_{Ic} (MPa m$^{1/2}$)		G_{Ic} (kJ/m^2)	
	RT	77 K	RT	77 K
Accura 25	0.94±0.15	1.59±0.33	0.55±0.15	0.53±0.20
ULTEM 9085 xy	3.53±0.18	5.83±0.72	6.02±0.75	10.1±2.29
ULTEM 9085 xz	3.70±0.34	7.00±0.61	7.30±1.17	14.1±2.34
ULTEM 9085 zx	1.62±0.23	1.71±0.70	1.92±0.49	1.32±0.65
PEEK xy	5.90±0.45	6.62±0.86	15.0±3.27	12.2±3.05
PEEK xz	4.41±0.88	5.92±1.72	7.50±2.74	9.90±4.28
PEEK zx	1.87±0.42	2.32±0.17	2.59±0.73	2.18±0.24
Helios PEEK xy	4.97±0.15	5.44±1.17	5.64±0.35	5.27±1.75
Helios PEEK xz	2.03±1.00	5.02±1.00	1.91±0.99	8.74±3.32
Helios PEEK zx	1.28±0.20	1.43±0.51	0.77±0.20	0.85±0.48

3.4 Irradiation induced degradation of the maximum short beam bending stress

The effect of irradiation has been assessed by three-point bending tests is short beam configuration. The ductility and strain at fracture of the thermosets RG35 and Accura 25 increases with dose up to 10 MGy (Figure 4). The Accura 25 modulus and ultimate stress decreases strongly already after 2 MGy gamma irradiation in ambient air.

IOP Conf. Series: Materials Science and Engineering **1327** (2025) 012210 doi:10.1088/1757-899X/1327/1/012210

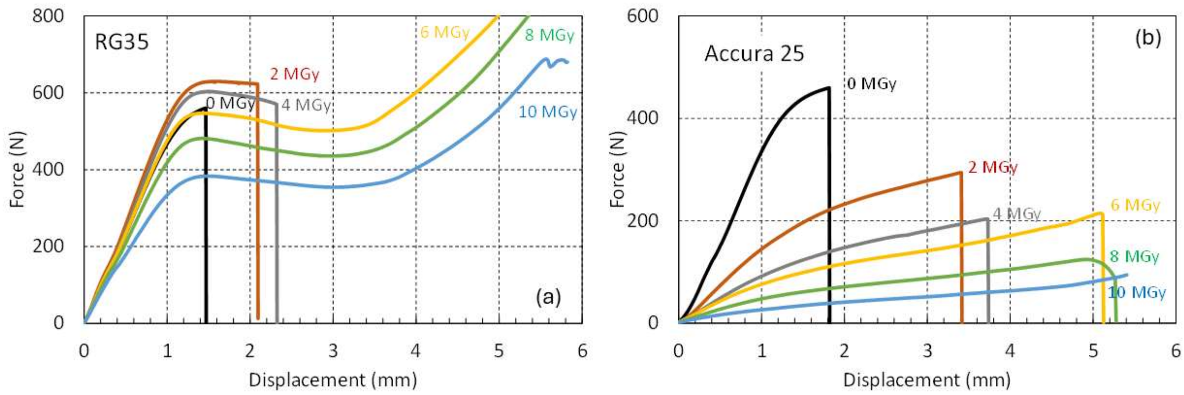

Figure 4. Short beam force vs displacement curves of (a) RG35 and (b) Accura 25 measured at RT before and after irradiation up to 10 MGy.

The T_g and short beam strength evolutions as a function of absorbed dose are presented in Figure 5(a) and Figure 5(b), respectively. For the FDM printed materials the three print orientations are compared. The PEEK samples printed in the xz direction did not break during the short beam bending test, and therefore, results are not included in Figure 5(b). PEEK and Helios PEEK printed in xy and xz directions retain comparatively high short beam strength up to 10 MGy. The ULTEM 9085 short beam strength is strongly reduced already after a dose of 5 MGy. Among the SLA printed resins RG 35 has outstanding radiation hardness.

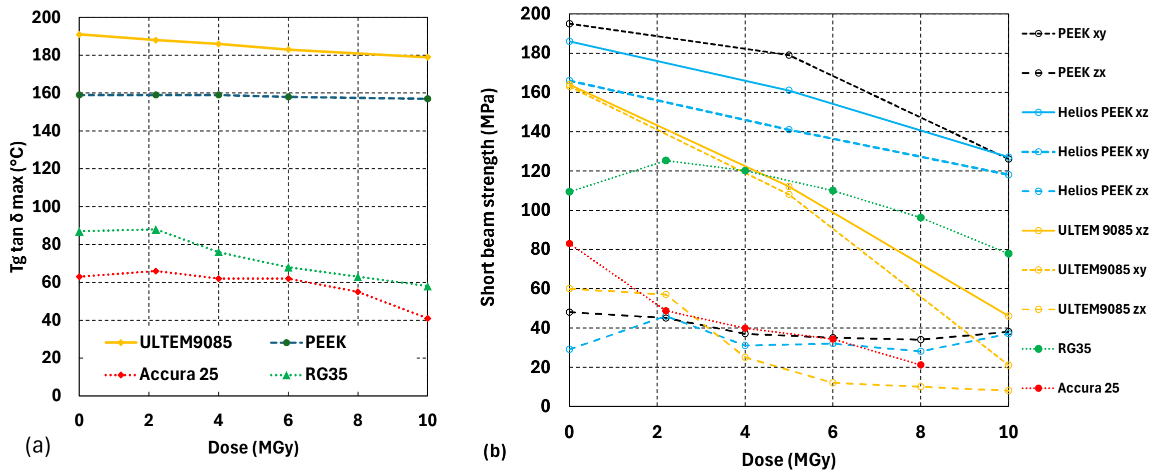

Figure 5. PEEK, Helios PEEK, ULTEM9085, RG35 and Accura 25 (a) T_g (tan δ max) and (b) short beam strength as a function of dose.

4. Discussion and conclusion

Materials properties of the three FDM materials studied are strongly anisotropic. PEEK printed in the on edge (xz) direction reaches very high bending stresses, comparable to those of extruded PEEK, showing the full potential of this material. However, the flexural stress of the PEEK samples printed in the upright (zx) direction did not exceed 50 MPa, even at 77 K. By optimising the printing parameters to approve the adhesion between the layers, it is probably possible to improve the mechanical strength in zx direction.

The T_g onset of the SLA printed epoxy resins is close to ambient temperature, and at RT their mechanical properties are lower than those of the FDM thermoplastics ULTEM 9085, PEEK and the charged Helios PEEK printed in xy and xz directions. However, the flexural strength of the isotropic SLA printed resins exceeds the strength of the FDM samples in zx direction.

Of the materials compared in this study, FDM printed PEEK exhibits highest radiation hardness. The FDM printed ULTEM 9085 properties are strongly degraded when the absorbed dose exceeds 5 MGy. The SLA printed thermoset RG35 keeps comparatively good mechanical properties up to 10 MGy. After a dose of 4 MGy the Accura 25 mechanical strength is reduced by about 50%.

The effect of irradiation in liquid helium, as it occurs during operation of superconducting magnets in particle accelerators, is subject of further studies. It is likely that irradiation damage rates of 3D printed polymers are reduced under such conditions [9].

Acknowledgements

We would like to thank Sébastien Clement and Jean-Sébastien Rigaud from the CERN Polymer Laboratory for their advice about 3D printing techniques and materials.

References

[1] Accura 25, technical data sheet, https://www.3dsystems.com/sites/default/files/2020-11/3d-systems-accura-25-datasheet-usen-2020-09-23-a-print.pdf
[2] Ultracur3D RG35 technical data sheet, https://move.forward-am.com/hubfs/LFS%20Documentation/Rigid%20Line/RG%2035/Preliminary_TDS_Ultracur3D_RG_35B_V1.1.pdf
[3] Roboze Helios™PEEK 2005, Technical data sheet, VERSION 1.0 _ REVISION DATE 04/02/2022
[4] A. Bagsik, V. Shoppner, "Mechanical Properties of Fused Deposition Modeling Parts Manufactured with Ultem 9085", Proceedings of ANTEC Conference, May 1-5, Boston, MA (2011)
[5] E. Padovano, M. Galfione, P. Concialdi, G. Lucco,C. Badini, "Mechanical and Thermal Behavior of Ultem® 9085 Fabricated by Fused-Deposition Modeling",
[6] Parragh, D.M.; Scheuerlein, C.; Piccin, R.; Ravotti, F.; Pezzullo, G.; Ternova, D.; Taborelli, M.; Lehner, M.; Eisterer, M. Irradiation Induced Aging of Epoxy Resins for Impregnation of Superconducting Magnet Coils. IEEE Trans. Appl. Supercond. 2024, 34, 7800107. https://doi.org/10.1109/TASC.2023.3332705.
[7] ASTM D4065; Standard Practice for Plastics: Dynamic Mechanical Properties: Determination and Report of Procedures. ASTM International: West Conshohocken, PA, USA, 2020.
[8] ASTM D7028-07; Standard Test Method for Glass Transition Temperature (DMA Tg) of Polymer Matrix Composites by Dynamic Mechanical Analysis (DMA). ASTM International: West Conshohocken, PA, USA, 2015.
[9] D.M. Parragh, C. Scheuerlein, N. Martin, R. Piccin, F. Ravotti, G. Pezzullo, T. Koettig, D. Lellinger, "Effect of irradiation environment and temperature on aging of epoxy resins for superconducting magnets", Polymers 2024, 16(3), 407
[10] ISO 527, "Plastics — Determination of tensile properties": https://www.iso.org/standard/75824.html
[11] ISO 178 "Plastics – Determination of flexural properties": https://www.iso.org/standard/70513.html
[12] ISO 14130:1997. "Fibre-reinforced plastic composites - Determination of apparent interlaminar shear strength by short-beam method" https://www.iso.org/standard/23642.html
[13] ISO 13586. "Plastics — Determination of fracture toughness (GIC and KIC) — Linear elastic fracture mechanics (LEFM) approach": https://www.iso.org/standard/67721.html
[14] G. Kirby et al, "Experimental Data and Fits for the Thermal Contraction of Future Magnet Materials at Cryogenic Temperatures", CERN, February 2016
[15] Plastics- Methods for determining the density of non-cellular plastics- Part 1: Immersion method, liquid pycnometer method and titration method" (DIN EN ISO 1183-1:2019)).
[16] Plastics- Determination of hardness- Part 1: Ball indentation method DIN EN ISO 2039- (2003-06)) ISO 2039-16))
[17] A. Gaarud, C. Scheuerlein, D.M. Parragh, S. Clement, J. Bertsch, C. Urscheler, R. Piccin, F. Ravotti, G. Pezzullo, R. Lach, "Fracture toughness, radiation hardness and processibility of polymers for superconducting magnets" Polymers 2024, 16(9), 1287